frontiers | Frontiers in Nanotechnology

ORIGINAL RESEARCH
published: 23 May 2022
doi: 10.3389/fnano.2022.888444

Diospyros malabarica Fruit Extract Derived Silver Nanoparticles: A Biocompatible Antibacterial Agent

*Shakil Ahmed Polash[1†], Amir Hamza[2†], Md. Monir Hossain[2], Mehedi Hasan Tushar[2], Masato Takikawa[3], Razib Datta Shubhra[2], Noshin Saiara[2], Tanushree Saha[4,5], Shinji Takeoka[6] and Satya Ranjan Sarker[2]**

[1]NanoBiosensing Research Laboratory (NBRL), School of Science, RMIT University, Melbourne, VIC, Australia, [2]Department of Biotechnology and Genetic Engineering, Jahangirnagar University, Dhaka, Bangladesh, [3]Department of Advanced Science and Engineering, Waseda University (TWIns), Tokyo, Japan, [4]Department of Textile Engineering, Dhaka University of Engineering and Technology, Gazipur, Bangladesh, [5]School of Engineering, RMIT University, Melbourne, VIC, Australia, [6]Department of Life Science and Medical Bioscience, Graduate School of Advance Science and Engineering, Waseda University (TWIns), Tokyo, Japan

OPEN ACCESS

Edited by:
Ajeet Kaushik,
Florida Polytechnic University,
United States

Reviewed by:
Avtar Singh,
Molekule Inc., United States
Dongmei Dong,
Florida International University,
United States

***Correspondence:**
Satya Ranjan Sarker
satya.sarker@bgeju.edu.bd

[†]These authors have contributed equally to this work

Specialty section:
This article was submitted to Biomedical Nanotechnology, a section of the journal Frontiers in Nanotechnology

Received: 02 March 2022
Accepted: 08 April 2022
Published: 23 May 2022

Citation:
Polash SA, Hamza A, Hossain MM, Tushar MH, Takikawa M, Shubhra RD, Saiara N, Saha T, Takeoka S and Sarker SR (2022) Diospyros malabarica Fruit Extract Derived Silver Nanoparticles: A Biocompatible Antibacterial Agent. Front. Nanotechnol. 4:888444. doi: 10.3389/fnano.2022.888444

Biogenic silver nanoparticles demonstrate excellent antibacterial activity against a broad range of bacteria. Herein, aqueous biogenic silver nanoparticles (Aq@bAgNPs) and ethanolic biogenic silver nanoparticles (Et@bAgNPs) were synthesized using aqueous as well as ethanolic extracts of *Diospyros malabarica* fruit, respectively. The as-prepared biogenic silver nanoparticles (bAgNPs) were characterized using UV-Vis, FTIR as well as energy dispersive X-ray (EDS) spectroscopy, electron microscopy, dynamic light scattering spectroscopy (DLS), and zetasizer. The zeta potentials of Aq@bAgNPs and Et@bAgNPs were −9.8 ± 2.6, and −12.2 ± 1.9 mV, respectively. The antibacterial activity of bAgNPs was investigated against seven bacterial strains (i.e., pathogenic and nonpathogenic) and Et@bAgNPs exhibited the highest antibacterial propensity (i.e., 20 nm in diameter) against *Bacillus subtillis* through disk diffusion assay. The trypan blue dye exclusion assay also confirmed the antibacterial propensity of as-prepared bAgNPs. Furthermore, both Aq@bAgNPs and Et@bAgNPs oxidize bacterial membrane fatty acids and generate lipid peroxides which eventually form complexes with thiobarbituric acid (i.e., malondialdehyde-thiobarbituric acid adduct) to bring about bacterial death. Both the nanoparticles demonstrated good hemocompatibility against human as well as rat red blood cells (RBCs). In addition, they exhibited excellent biocompatibility *in vivo* in terms of rat liver (i.e., serum ALT, AST, and γ-GT) and kidneys (i.e., serum creatinine) function biomarkers.

Keywords: *Diospyros malabarica*, antibacterial activity, lipid peroxidation, hemocompatibility, biocompatibility

1 INTRODUCTION

Nowadays bacterial infection has become a real threat to public health (Abuelizz et al., 2021). The misuse and overuse of commercial antibiotics has led to the development of drug-resistant bacteria. Mutations as well as lateral gene transfer play a vital role in contributing the emergence of drug-resistant bacterial species (Shriram et al., 2018; Polash et al., 2021). On the other hand, antibiotics are usually effective for a certain period of time and, therefore, they need to be taken continuously for

effective treatment (Braine, 2011; Han et al., 2019). In this circumstance, it is high time to develop new antibacterial agent(s) having broad-spectrum antibacterial activity to replace the commercially available antibiotics to kill the pathogenic as well as drug resistant bacteria (Dhau et al., 2021; Singh et al., 2022).

Nanoparticles (NPs) can be a suitable alternative to antibiotics in the current fight against bacteria. Among different classes of NPs, the metal-based inorganic NPs including gold (Zhang et al., 2015), silver (Durán et al., 2016), copper (Kruk et al., 2015), zinc oxide (Król et al., 2017), and graphene oxide nanoparticles (Aunkor et al., 2020) have excellent physical and chemical properties and have been used to inhibit the growth of bacteria due to their antimicrobial propensity. They demonstrate broad-spectrum antibacterial activity, and the development of bacterial resistance is very difficult due to their non-specific antibacterial mechanisms (Sánchez-López et al., 2020). Among them, silver nanoparticles (AgNPs) are widely used in pharmaceutical products (Mathur et al., 2018), cosmetics (Gajbhiye and Sakharwade, 2016), wastewater treatment (Kaegi et al., 2011), wound healing agents (Chai et al., 2018), and so on. However, chemically synthesized AgNPs are highly unstable because of their aggregation tendency that results in the oxidation of silver atoms (Levard et al., 2012; de Oliveira and Cardoso, 2014). The aggregated AgNPs lose their antibacterial activity (Bélteky et al., 2019) and the silver ions leaked from AgNPs bring about health hazard as well as environmental pollution (Ramalingam et al., 2016). Moreover, the chemical synthesis of NPs is troublesome, expensive, and requires chemical reagents (e.g., $NaHB_4$, citric acid, and so on) that are hazardous for the environment. To address these issues, plant extract has been used as an alternative reducing agent to reduce Ag^+ to Ag^0 to synthesize AgNPs. Phytoconstituents present in the plant extract act as reducing agents and reduce silver nitrate ($AgNO_3$) in an easy, fast, cost-effective, and eco-friendly manner (Poulose et al., 2014). The presence of phytoconstituents in the plant extract mainly depends on the extraction solvent. It was reported that polar solvents usually extract most of the constituents of plant parts including alkaloids, phenols, flavonoids, terpenoids, tannins, and andrographolides (Mondal et al., 2017; Masum et al., 2019). The phytochemicals have antioxidant, anticancer, anti-inflammatory, antidiabetic, and antimicrobial activities (Mujeeb et al., 2014; Haq et al., 2019; Kausar et al., 2021).

Diospyros malabarica is a flowering tree and natively grown in the South-East region of Asia. The fruit extract has been used as therapeutics to cure a wide range of diseases including diabetics since ancient times (Ghosh et al., 2022). Furthermore, it was also used to synthesize AgNPs through green approach to reduce the consumption of chemical reagents. Previous study also supports that phytoconstituents present in the fruit extracts mediate the synthesis of AgNPs at room temperature (Bharadwaj et al., 2021). During the synthesis process, phytochemicals of the plant extracts play a critical role in reducing $AgNO_3$ to form colloidal AgNPs (He et al., 2016). However, the antibacterial propensity of *D. malabarica* derived biogenic AgNPs (bAgNPs) has not been extensively investigated against pathogenic bacteria. On the other hand, a detailed investigation on the biocompatibility as well as antibacterial propensity of biogenic AgNPs against a wide range of pathogens need to be performed to understand the wide scale applicability of the particles.

In this study, biogenic AgNPs (bAgNPs) were synthesized using aqueous and ethanolic extract of *D. malabarica* fruit. The as-synthesized bAgNPs were then characterized by UV-vis spectroscopy, powder X-ray diffractometer (XRD), Fourier transform infrared (FTIR) spectroscopy, transmission and scanning electron microscopy, and energy dispersive X-ray analysis (EDX). The maximum absorption of aqueous and ethanolic extract derived nanoparticles at 428 and 416 nm confirmed the successful generation of aqueous biogenic AgNPs (Aq@AgNPs) and ethanolic biogenic AgNPs (Et@AgNPs), respectively. XRD and FTIR confirmed the presence of silver nanocrystals as well as the chemical composition of the as-synthesized nanoparticles. Moreover, the morphology of nanoparticles was determined using electron microscopy and zeta size analyzer was used to measure the hydrodynamic size as well as zeta potential of the biogenic AgNPs. The antibacterial potential of as-prepared bAgNPs was investigated against pathogenic as well as non-pathogenic bacterial strains through broth dilution and disk diffusion assay to determine the minimum inhibitory concentration (MIC) and diameter of the inhibitory zone (in millimeters), respectively. The lipid peroxidation (LPO) assay was also performed to investigate their mechanism of antibacterial propensity. To investigate the biocompatibility of *D. malabarica* fruit extract derived bAgNPs, hemocompatibility of the nanoparticles was investigated using human as well as rat red blood cells (RBCs). Furthermore, the biocompatibility of as-prepared bAgNPs was also investigated *in vivo* using Wister rats through measuring the level of serum aspartate aminotransferase (AST), alanine aminotransferase (ALT), and gamma-glutamyl transferase (γ-GT) as biomarkers of liver function and serum creatinine as biomarker of renal function.

2 MATERIALS AND METHODS

2.1 Materials

Silver nitrate ($AgNO_3$), ethylenediaminetetraacetic acid (EDTA), potassium bromide (KBr), and ethanol were purchased from Sigma-Aldrich (USA). Peptone, yeast extract, and sodium chloride were collected from Unichem (China). Trypan blue dye was purchased from Alfa Aesar (United Kingdom). Agar powder was purchased from Titan Biotech Ltd. (India). Trichloroacetic acid (TCA) was purchased from Merck (Germany) and thiobarbituric acid (TBA) was bought from JT Baker (USA). Biochemical assay kits for serum AST, ALT and γ-GT were purchased from Vitro Scient (Egypt). On the other hand, serum creatinine assay kit was bought from Crescent Diagnostics (The Kingdom of Saudi Arabia). Both pathogenic (i.e., *S. typhi*, *S. aureus*, *V. cholerae*, enteropathogenic *Escherichia coli* (EPEC), and *E. faecalis*), and nonpathogenic (i.e., *E. coli* DH5α, and *B. subtilis* RBW) bacterial strains were obtained from the Department of Biotechnology and Genetic Engineering,

Jahangirnagar University, Savar, Dhaka 1342, Bangladesh. Twenty-five Wistar male rats (weighing ~60 g) were obtained from the Department of Biochemistry and Molecular Biology, Jahangirnagar University, Dhaka, Bangladesh.

2.2 Synthesis of Biogenic Ag Nanoparticles

Both aqueous and ethanolic extracts of *D. malabarica* fruit were used to prepare biogenic Ag nanoparticles (bAgNPs). The fruit extracts were prepared according to our previously published protocol (Shubhra et al., 2019; Shubhra et al., 2021). A freshly prepared $AgNO_3$ (10 mM) solution was added separately to aqueous (Aq) and ethanolic (Et) fruit extracts at a ratio of 9:1 (ml). The mixtures of $AgNO_3$ solution and fruit extracts were incubated in the dark at 30°C for 24 h upon constant stirring. Here, the plant extracts act as reducing agents, and the transformation of colorless $AgNO_3$ solution into brown color confirms the reduction of Ag^+ to Ag^0 (Ahmed et al., 2016; Niloy et al., 2020). The unreacted plant extracts as well as $AgNO_3$ were removed through centrifugation at 16,000xg for 60 min. The supernatant was discarded, and the bAgNPs generated by the aqueous as well as ethanolic extracts were washed twice with distilled water before redispersing in distilled water.

2.3 Characterization

UV-visible spectrophotometer (Specord® 205, Analytik Jena, Germany) was used to characterize the as-synthesized biogenic AgNPs. FTIR spectroscopy (IRPrestige-21, SHIMADZU, Japan) and powder X-ray diffractometer (GNR X-Ray Explorer, Italy) equipped with Cu K_α (0.154 nm) at 25 mA were used to characterize the chemical and crystal property of bAgNPs, respectively. The XRD spectrum was obtained by scanning the diffraction angle (2θ) region at 30 kV. The diffraction angle varied in the range of 10–50° and the scanning rate was 5°/s. The morphology and the composition of biogenic nanoparticles were characterized using TEM having a field emission gun (HF-2200; Hitachi, Tokyo, Japan) coupled with energy-dispersive X-ray spectroscopy (EDAX Genesis; AMETEK, Pennsylvania, United States) operating at 200 kV. The hydrodynamic size and zeta potential of bAgNPs were measured using a zeta size analyzer (Nano-ZS90; Spectris PLC, Egham, U.K.).

2.4 Antibacterial Activity Assay

The antibacterial activity of as-synthesized biogenic AgNPs was investigated against five pathogenic (i.e., *S. typhi*, *S. aureus*, *V. cholerae*, EPEC, and *E. faecalis*) and two non-pathogenic (i.e., *E. coli* DH5α, and *B. subtilis* RBW) bacterial strains. The chosen strains include both Gram-positive and negative bacterial strains. The antibacterial activity of both aqueous and ethanolic extract mediated biogenic AgNPs was determined through MIC and disc diffusion assay, and trypan dye exclusion assay (Polash et al., 2017b; Hossain et al., 2019).

2.4.1 Minimum Inhibitory Concentration

The MIC values were determined through broth dilution method to get the minimum amount of Aq@AgNPs, and Et@AgNPs required to inhibit the growth of a particular bacterial strain. The MIC values of both Aq@AgNPs, and Et@AgNPs against the tested bacterial strains were determined according to our previously reported protocol (Polash et al., 2017a).

2.4.2 Zone of Inhibition

The antibacterial activity of Aq@AgNPs as well as Et@AgNPs was determined following our previously reported disk diffusion assay protocol (Polash et al., 2017a). Briefly, metrical filter paper disks containing 80 μg of bAgNPs were placed on the LB agar plates containing uniformly spread bacteria. The LB agar plates were then incubated for optimal growth (i.e., 16 h at 37°C). The antibacterial activity was determined by measuring the diameter of clear zones surrounding the filter paper disks using slide callipers.

2.4.3 Trypan Blue Dye Exclusion Assay

Trypan blue is a negatively charged dye and cannot penetrate the intact bacterial cell wall. However, the dead cells can absorb the blue pigment through the damaged cell membrane. The trypan blue dye exclusion assay was performed according to our previously established protocol with little modifications (Ranjan Sarker et al., 2019). Briefly, 20 μL (1 μg/μL) of Aq@AgNPs and Et@AgNPs was mixed separately with 80 μL of overnight grown culture (1×10^6 CFU/ml) of the respective bacterial strains and incubated at 37°C and 120 rpm for 1.5 h. The images of live and dead bacterial cells were taken using a phase contrast microscope.

2.5 LPO Assay

The peroxidation potential of bacterial lipid membrane by Aq@AgNPs and Et@AgNPs was investigated according to our previously established protocol (Ranjan Sarker et al., 2019). Briefly, TCA solution (10%) was added to bAgNPs-treated bacterial suspension and the insoluble cellular components were separated through centrifugation to collect the supernatant. The supernatant was centrifuged again to precipitate any remaining proteins and cellular debris. Malondialdehyde (MDA), a polyunsaturated fatty acid, presents in the supernatant reacts with the freshly prepared TBA (0.67%) solution and produce MDA-TBA adduct when incubated in a hot water bath for 10 min. The adduct was then cooled down to room temperature before measuring the absorbance at 532 nm by a UV-visible spectrophotometer.

2.6 *In Vitro* Hemocompatibility Assay

The compatibility of human and rat erythrocytes with bAgNPs (i.e., Aq@AgNPs and Et@AgNPs) was investigated according to our previously established protocol (Ranjan Sarker et al., 2019; Sarker et al., 2022). Briefly, human and rat red blood cells (RBCs) were isolated from serum through centrifugation at 500 *g* for 10 min. The serum was then removed before resuspending RBCs in 5 ml phosphate-buffered saline (PBS) and centrifuged again. The cell suspension was washed twice with 150 mM NaCl solution at 3,000 g for 3 min. Finally, 0.1 ml of RBCs solution was mixed with 0.4 ml of various amounts of bAgNPs (i.e., 20, 40, 60, and 80 μg) and incubated for 30 min at 37°C and 150 rpm before centrifuging at 1,377 g for 5 min. The supernatant was

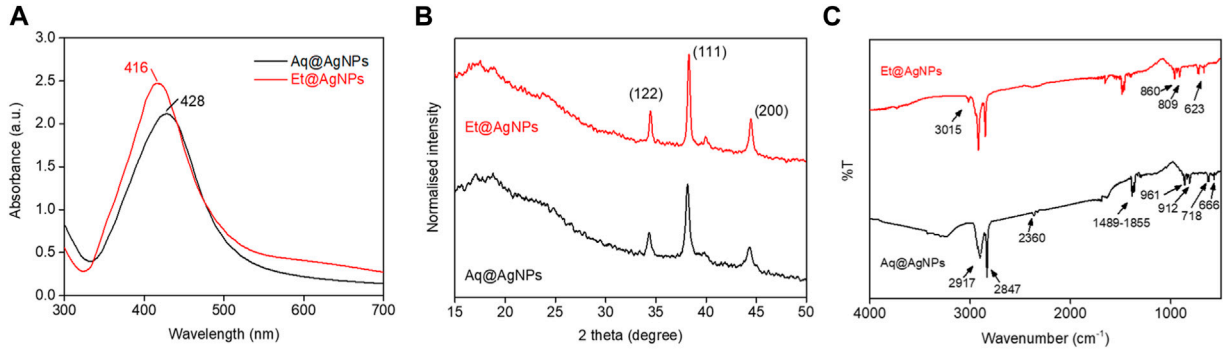

FIGURE 1 | Characterization of as-prepared biogenic AgNPs using the aqueous (Aq) and ethanolic (Et) fruit extract of *Diospyros malabarica*. **(A)** UV-visible spectra of aqueous extract mediated AgNP (i.e., Aq@AgNPs) and ethanolic extract mediated AgNP (i.e., Et@AgNPs). **(B)** Crystallinity study of Aq@AgNPs and Et@AgNPs by powder XRD. **(C)** Analysis of chemical composition of Aq@AgNPs and Et@AgNPs by FTIR.

taken out to measure its optical density at 570 nm. Herein, erythrocytes incubated with PBS and water were considered as negative and positive controls, respectively. The hemolysis rate was calculated using the following formula:

$$\%\ of\ hemolysis = \frac{absorbance\ of\ sample - absorbance\ of\ negative\ control}{absorbance\ of\ positive\ control - absrobance\ of\ negative\ control} \times 100$$

2.7 Cytotoxicity Study

Wistar male rats were used to investigate the toxicity of bAgNPs *in vivo*. Twenty-five rats were divided into five groups (5 per group) and were maintained in a hygienic environment followed in our previous study (Hossain et al., 2019). Two doses of Aq@AgNPs and Et@AgNPs (i.e., 3 and 6 mg/kg of rat body weight) were delivered intravenously via the tail vein. After 7 days, about 3 ml of blood was collected and the serum was separated through centrifugation at 538 *g* for 10 min at room temperature.

To determine whether biogenic Aq@AgNPs and Et@AgNPs have any toxic effects on rat tissues, the concentration of several biomarkers was measured. Serum alanine aminotransferase (ALT), aspartate aminotransferase (AST), and gamma-glutamyltransferase (γ-GT) were measured as liver function biomarker. On the other hand, the level of serum creatinine was measured as kidney function biomarker. The concentration of all the biomarkers was determined according to the instructions provided with the reagent kit. All the animal experiments performed in the study were approved by the Biosafety, Biosecurity & Ethical Committee of Jahangirnagar University [BBEC, JU/M 2019(4)1].

3 RESULTS AND DISCUSSION

3.1 Characterization of Biogenic AgNPs

The colorless $AgNO_3$ solution turned brown after the addition of *D. malabarica* (aqueous and ethanolic) fruit extract confirming the reduction of Ag^+ to Ag^0. The change of color is due to the presence of secondary metabolites especially phenols, flavonoids, and andrographolides in *D. malabarica* fruit extract. These secondary metabolites act as reducing agents. They also bind to the surface of the biogenic nanoparticles as capping agents. The UV-visible spectra confirm the generation of biogenic AgNPs since the λ_{max} of Aq@AgNPs and Et@AgNPs are 428 and 416 nm, respectively (**Figure 1A**). The data are in the same line with the previously published literature that showed the surface plasmon resonance (SPR) value of AgNPs is 420 nm (Ramalingam et al., 2016; Hossain et al., 2019). The SPR is very specific for metals as it exhibits strong scattering and absorption properties of AgNPs by causing collective oscillation when electrons on the metal surface are excited by light at a specific wavelength (Li et al., 2010).

The crystalline structure of the as-synthesized Aq@AgNPs and Et@AgNPs was investigated by powder XRD. The analysis of XRD spectra of as-synthesized bAgNPs showed diffraction peaks at 32.2°, 38.3°, and 44.4° (**Figure 1B**) that can be assigned to the planes (122), (111), and (200) facets of Ag crystal, respectively (Ashraf et al., 2016; Goudarzi et al., 2016). On the other hand, FTIR spectroscopy was carried out to confirm the presence of secondary metabolites in the fruit extracts as well as in the as-synthesized bAgNPs, since the secondary metabolites (e.g., alkaloids, flavonoids, and so on) are responsible for the reduction of Ag^+ and stabilization of bAgNPs (Elamawi et al., 2018; Hossain et al., 2019). Absorption bands at 3,015, (2917 and 2847), 2360, 1489–1855, (961 and 912), and (718 and 666) cm^{-1} were attributed to symmetric CH_2 stretching, C-H asymmetric stretching, C≡C stretching, carbonyl group, C-OH stretching, and C-H stretching of the aromatic compound in Aq@AgNPs and Et@AgNPs (**Figure 1C**). FTIR spectra of all the precursor compounds are available in **Supplementary Figure S1**.

The average hydrodynamic diameter of Et@AgNPs was larger than that of Aq@AgNPs (**Figure 2A**). The hydrodynamic diameters of Aq@AgNPs and Et@AgNPs were 287 ± 117 and 375 ± 69 nm, respectively. Moreover, the zeta potentials of Aq@AgNPs and Et@AgNPs were −9.8 ± 2.6 and −12.2 ± 1.9 mV, respectively (**Figure 2B**). The negative zeta potential of bAgNPs is due to the adsorption of bioactive molecules on the particle

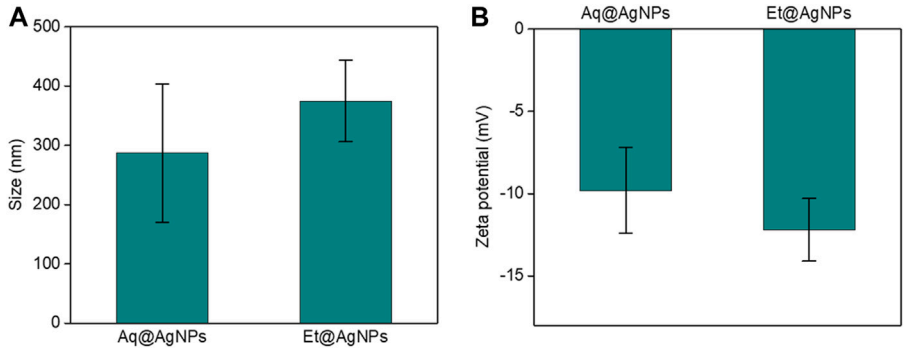

FIGURE 2 | Determination of **(A)** size and **(B)** surface potential of Aq@AgNPs and Et@AgNPs.

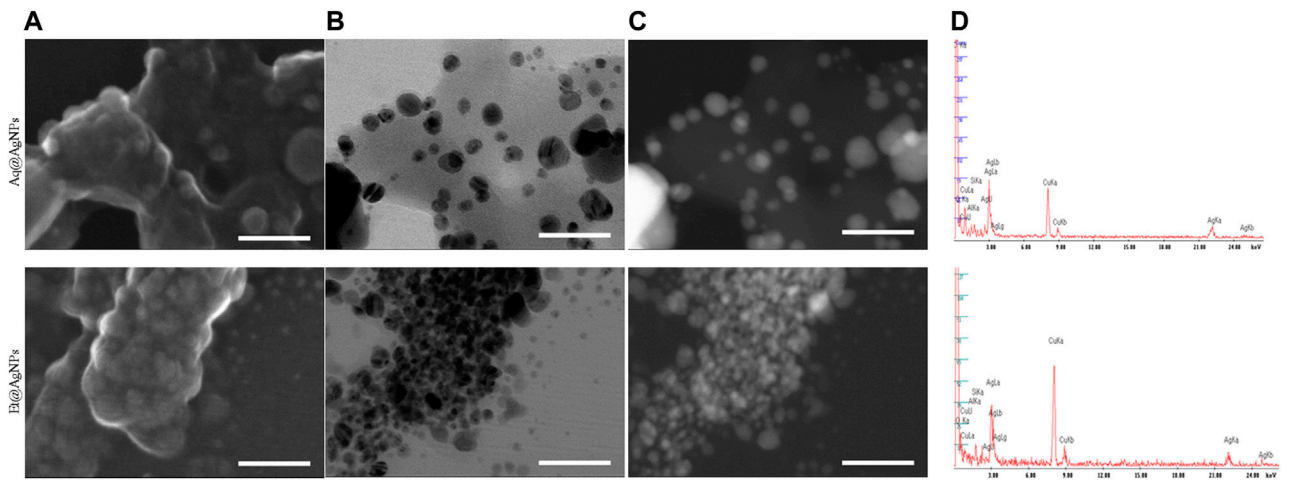

FIGURE 3 | Analysis of the shape and morphology of biogenic Aq@AgNPs using scanning TEM. **(A)** SE images indicated biogenic polymers composing the surface of NPs. **(B)** Scanning TEM and **(C)** HAADF images (Z-contrast images) revealed the presence of bAgNPs coated with polymers (x500 k). **(D)** Peaks in 2–4 keV in EDX analysis confirmed that the constituent element included Ag. Scale bar: 60 nm.

surface (Rao and Paria, 2015). On the other hand, the polarity of solvents used to extract phytoconstituents from *D. malabarica* fruits plays an important role, since the chemical structure of secondary metabolites differs from each other. Hence, the composition of aqueous fruit extract differs from that of ethanolic extracts. The different chemical composition of different solvent extracts influences the surface potential of as-synthesized bAgNPs.

The shape and morphology of biogenic Aq@AgNPs and Et@AgNPs were determined using a scanning transmission electron microscope (STEM) (**Figure 3**). STEM images confirmed that bAgNPs were surrounded by polymers and difficult to observe directly. In addition, TEM or High-angle annular dark-field (HAADF) images also exhibited that bAgNPs were coated with polymers and most of the NPs were spherical. EDS analysis confirmed that both NPs were composed of Ag, C, and O (**Figure 3**). A characteristic Ag peak was observed at ~3 keV. Other peaks such as Cu and Si are due to artifacts of TEM grid and vacuum pump silicone oil analysis, respectively. Hence, it can be concluded that bAgNPs are coated with bioactive polymers present in the fruit extracts of *D. malabarica*.

3.2 Antimicrobial Activity Assay

The broth dilution method was used to estimate the MIC values of as-synthesized Aq@AgNPs as well as Et@AgNPs. In the case of Aq@AgNPs, the lowest MIC value was 0.25 μg/ml against *S. typhi*, *E. faecalis*, *E. coli* DH5α, and *V. cholerae* (**Table 1**). On the other hand, the lowest MIC value (i.e., 0.125 μg/ml) for Et@AgNPs was found against *B. subtilis* and *S. aureus* (**Table 1**). A clear zone on the agar media surrounding the sterile metrical filter paper disk confirmed the antibacterial/bactericidal activity of as-synthesized bAgNPs. The highest antibacterial activity of Aq@AgNPs and Et@AgNPs (amount: 80 μg) was observed against *E. faecalis* (ZOI: 17.77 mm) and *B. subtilis* (ZOI: 20 mm), respectively (**Table 1**). On the other hand, the lowest antibacterial activity of Aq@AgNPs (13.22 mm) and Et@AgNPs (15.89 mm) was observed against enteropathogenic *E. coli* or EPEC. Aqueous fruit extract, ethanolic fruit extract, and silver nitrate were used as control,

TABLE 1 | Minimum inhibitory concentration (MIC) as well as the zone of inhibition (ZOI) of the as-synthesized bAgNPs against different bacteria.

Tested strains	MIC (μg/ml)		Inhibitory zone (mm)					Pathogenicity
	Aq@AgNPs	Et@AgNPs	Aq extract	Aq@AgNPs	Et extract	Et@AgNPs	$AgNO_3$	
B. subtilis	0.50	0.125	7 ± 0	14.9 ± 0.67	6.5 ± 0.0	20.0 ± 0.67	8.0 ± 0.0	Non-pathogenic
S. typhi	0.25	0.25	7.5 ± 0	15.67 ± 0.30	7.5 ± 0.0	19.23 ± 0.70	7.0 ± 0.55	Pathogenic
E. facealis	0.25	0.25	7 ± 0	17.77 ± 0.50	6.0 ± 0.0	17.11 ± 0.50	7.0 ± 0.0	Pathogenic
EPEC	0.50	0.50	6.5 ± 0	13.22 ± 0.19	7.5 ± 0	15.89 ± 0.85	7.0 ± 0.0	Pathogenic
E. coli	0.25	0.25	7 ± 0	14.89 ± 0.70	7.5 ± 0	18.55 ± 0.70	9.0 ± 0.33	Non-pathogenic
V. cholerae	0.25	0.25	7.5 ± 0	14.23 ± 0.50	7.5 ± 0	18.33 ± 0.34	8.5 ± 0.0	Pathogenic
S. aureus	0.25	0.125	7 ± 0	14.67 ± 87	6.5 ± 0	18.78 ± 0.19	9.0 ± 0.0	Pathogenic

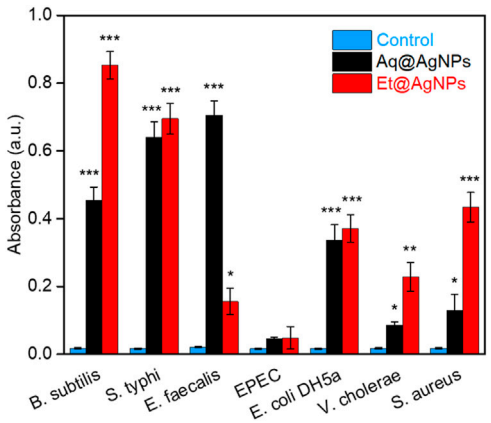

FIGURE 4 | Absorbance of MDA-TBA adduct at 532 nm (n = 3). The absorbance of MDA-TBA adduct of bAgNPs-treated bacteria was significantly higher than that of the untreated bacteria (i.e., control). Here, $*p < 0.05$ vs. control, $**p < 0.01$ vs. control, and $***p < 0.001$ vs. control.

and they showed lower antibacterial activity when compared to that of the as-synthesized bAgNPs against all the tested bacteria (**Table 1**).

The phytoconstituents of *D. malabarica* fruit extracts contain a variety of biologically active compounds including long chain hydrocarbons, hydroxyls, as well as carboxyl groups containing bioactive molecules that can act as the hydrophilic moieties. Therefore, noncovalent (i.e., hydrophobic) interactions between the bAgNPs and bacteria were responsible for the bacterial death. Increased uptake of the negatively charged Aq@AgNPs and Et@AgNPs is associated with their higher hydrophobicity when compared to that of the plant extracts and silver nitrate (Li et al., 2014; Hossain et al., 2019). The interaction between the bAgNPs and bacteria could also be due to molecular clustering effect (Arakha et al., 2015). Finally, the release of silver ions and/or their intracellular deposition is responsible for the antibacterial mechanism of bAgNPs (Kim et al., 2016; Hoseinnejad et al., 2018). The Ag^+ ions released from the as-synthesized bAgNPs can interact with sulfur as well as phosphorus containing proteins present in the plasma membrane as well as in the bacterial cell wall via electrostatic interactions and result in the formation of pores in the membrane (Hindi et al., 2009). The resultant membrane pores allow the outflow of bacterial intracellular contents and bring about bacterial death. Bharadwaj et al. (2021) reported the concentration-dependent antibacterial activity of bio-synthesized AgNPs where the diameter of the clear zone of inhibition (ZOI) was about 12–14 mm at 1,000 μg/ml concentration (Bharadwaj et al., 2021). Herein, we investigated the antibacterial activity of both Aq@AgNPs and Et@AgNPs using much lower concentration (amount: 80 μg). Our observed antibacterial activity in the presence of lower amount of nanoparticles indicates the promising antimicrobial potential of *D. malabarica* fruit extract derived biogenic AgNPs.

Trypan blue dye exclusion assay was performed to confirm the damage of bacterial cell wall due to interaction with bAgNPs. Hydrophobic interactions between the nanoparticles and bacterial cell wall were responsible for the membrane damage. As a result, blue dye deposited inside the bacterial cytosol and appeared blue under the phase contrast microscope (**Supplementary Figures S2–S8**). However, intact cell wall of live bacteria inhibits the dye from getting inside.

3.3 Lipid Peroxidation

To investigate the oxidative potential of bacterial membrane fatty acids by bAgNPs, we performed lipid peroxidation (LPO) assay. The MDA-TBA adduct was formed after the treatment of bacteria with Aq@AgNPs and Et@AgNPs due to their strong hydrophobic interactions with bacterial cell wall. The highest amount of MDA-TBA adduct was formed when Et@AgNPs was used to treat Gram-positive *B. subtilis* (**Figure 4**). On the other hand, the highest amount of MDA-TBA adduct was formed when *E. faecalis* were treated with Aq@AgNPs (**Figure 4**). Different amount of MDA-TBA adduct was formed when different bacterial strains were treated with bAgNPs. This is because of the differences in the membrane composition of different bacterial strains that influence their interaction with the nanoparticles. Thus, lipid peroxides are formed due to the oxidation of bacterial cell membrane fatty acids by the as-synthesized bAgNPs.

As transition metals (e.g., Ag) put oxidative stress on fatty acids, the reactive oxygen species (ROS) are generated after the treatment of bacterial cell membrane with bAgNPs (Li et al., 2012). The generated ROS oxidizes fatty acids in the bacterial membrane and produces lipid peroxides. Furthermore, ROS-mediated oxidative stress inhibits the electron transport chain and alters bacterial metabolic responses (Wang et al., 2017). Thus,

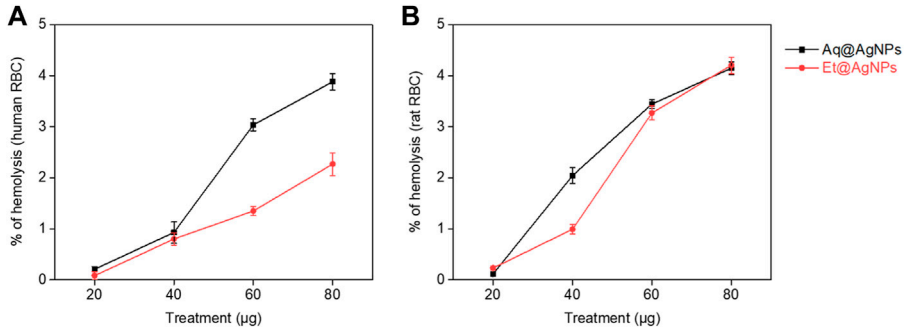

FIGURE 5 | Hemocompatibility of Aq@AgNPs and Et@AgNPs **(A)** human and **(B)** rat erythrocytes.

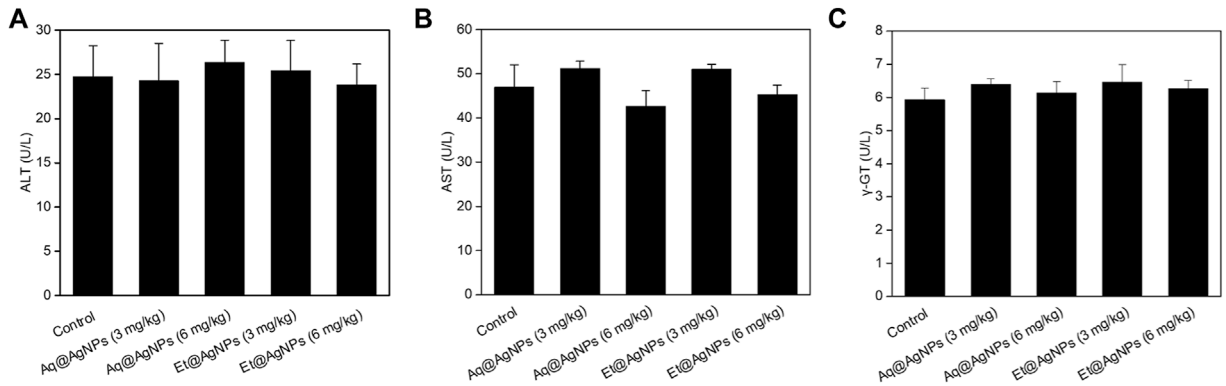

FIGURE 6 | Liver function biomarkers of bAgNPs-treated rats. Serum **(A)** alanine aminotransferase (ALT), **(B)** aspartate aminotransferase (AST), and **(C)** gamma-glutamyl transferase (γ-GT) were measured as liver function biomarkers. Two different doses (i.e., 3 and 6 mg/kg) of both Aq@AgNPs and Et@AgNPs were injected through intravenous route. No significant difference was observed in One-way ANOVA test when treatment groups were compared with that of the control and $p > 0.05$.

it induces apoptosis to the corresponding bacterial cells by stimulating the expression of apoptosis genes (Wang et al., 2017).

3.4 Hemocompatibility Assay

The compatibility of biogenic Aq@AgNPs and Et@AgNPs to human and rat RBCs was investigated in a dose-dependent manner (i.e., 20–80 µg). Both the nanoparticles showed excellent hemocompatibility to human as well as rat RBCs (**Figure 5**). The percentage of hemolysis in the presence of 80 µg Aq@AgNPs was 4.1 and 3.9% in the case of human and rat RBCs, respectively. On the other hand, the percentage of hemolysis in the presence of 80 µg Et@AgNPs was 4.2 and 2.3% in the case of human and rat RBCs, respectively. Biogenic Et@AgNPs showed greater compatibility to both human and rats RBCs than that of Aq@AgNPs. This could be due to greater negative surface potential (i.e., −12.2 ± 1.9 mV) of Et@AgNPs when compared that of Aq@AgNPs. The negative surface potential brings about stronger electrostatic repulsion with the negatively charged RBCs. In both cases, the percentage (%) of hemolysis was less than that of the therapeutically acceptable hemolytic value (i.e., 5%) (Nayak et al., 2016; Hossain et al., 2019; Sarker et al., 2022). Furthermore, the variation in hemolysis

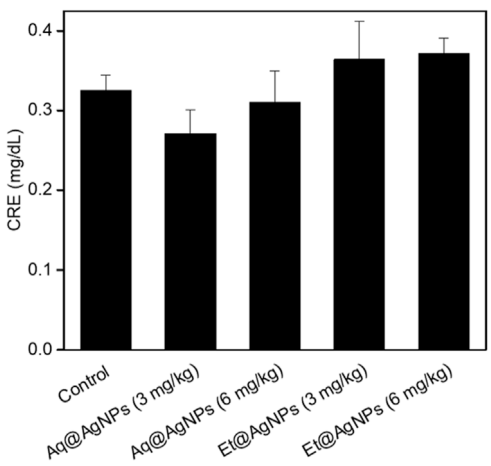

FIGURE 7 | Kidney function biomarker of bAgNPs-treated rats. Serum creatinine (CRE) was measured as a liver function biomarker. Two different doses (i.e., 3 and 6 mg/kg) of both Aq@AgNPs and Et@AgNPs were injected through intravenous route. No significant difference was observed in One-way ANOVA test when treatment groups were compared with that of the control and $p > 0.05$.

percentage is due to the differences in membrane composition of human and rat RBCs (da SilveiraCavalcante et al., 2015).

3.5 Liver and Kidney Function Biomarkers

Neither Aq@AgNPs nor Et@AgNPs showed any significant toxic effect on the liver (**Figure 6**) and kidney tissues (**Figure 7**) at both doses (3 and 6 mg/kg) of the biogenic nanoparticles. The colloidal AgNPs are usually deposited to the liver and kidneys and interfere with their functions (Kim et al., 2007; Ahmad and Zhou, 2017; Hossain et al., 2019). To determine the toxic effects of bAgNPs, liver function was investigated by measuring the level of serum ALT, AST, and γ-GT enzymes after the intravenous delivery of bAgNPs through tail vein. Any decrease in ATP level indicates damage of the liver tissues that causes the release of hepatic enzymes (i.e., ALT and AST) (Ramaiah, 2007; Hossain et al., 2019). On the other hand, γ-GT is a hepatobiliary enzyme whose level rises within hours of cholestasis (Ramaiah, 2007). Meanwhile, the toxic effect of bAgNPs on kidneys was also investigated by determining the level of serum creatinine. Low level of serum creatinine indicates the kidneys' ability to filter waste products from the blood and excrete them in the urine (Kaur et al., 2012).

Our data suggest that bAgNPs (up to 6 mg/kg) are therapeutically safe for the liver, since no statistically significant elevation of the level of serum biomarkers was observed. Furthermore, intravenous administration of different doses (up to 6 mg/kg) of bAgNPs for 7 days also did not show any significant elevation in the level of serum creatinine. Hence, both Aq@AgNPs and Et@AgNPs did not show any toxic effect to the liver and kidneys.

4 CONCLUSION

The biogenic AgNPs were synthesized using aqueous as well as ethanolic extract of *D. malabarica* fruit through green synthesis approach. The as-prepared nanoparticles were characterized through UV-visible, XRD, FTIR, electron microscopy, and EDX spectroscopy. The antimicrobial activity of Aq@AgNPs and Et@AgNPs (amount: 80 μg) was investigated against both pathogenic and non-pathogenic bacterial strains. Both Aq@AgNPs and Et@AgNPs showed enhanced antibacterial activity when compared to that of pure fruit extracts against all the tested bacteria. Lipid peroxidation assay confirmed the oxidation of bacterial membrane fatty acids resulting in the formation of membrane pores. This promotes the interaction of bAgNPs with DNA and other cellular macromolecules to kill bacteria. On the other hand, the as-synthesized bAgNPs showed excellent hemocompatibility and did not show any significant toxicity to liver and kidneys. Therefore, the broad-spectrum antibacterial potential and good biocompatibility of *D. malabarica* fruit extract derived bAgNPs can be recommended for future therapeutic applications.

DATA AVAILABILITY STATEMENT

The original contributions presented in the study are included in the article/**Supplementary Material**, further inquiries can be directed to the corresponding author.

ETHICS STATEMENT

The animal study was reviewed and approved by Jahangirnagar University.

AUTHOR CONTRIBUTIONS

All authors listed have made a considerable, direct and intellectual contribution to the work, and approved it for publication.

FUNDING

This research project was partially supported by Jahangirnagar University Research Grant 2018, University Grants Commission (UGC)-Jahangirnagar University Joint Research Grant 2019, Government of Bangladesh. SAP acknowledges National Science and Technology (NST) Fellowship (2018–2019) awarded by the Ministry of Science and Technology, Government of Bangladesh.

ACKNOWLEDGMENTS

The authors acknowledge Wazed Miah Science Research Center of Jahangirnagar University, Bangladesh and Waseda University Central Instrument Facility, School of Advanced Science and Engineering, Tokyo, Japan for allowing the use of their comprehensive facilities and services.

SUPPLEMENTARY MATERIAL

The Supplementary Material for this article can be found online at: https://www.frontiersin.org/articles/10.3389/fnano.2022.888444/full#supplementary-material

REFERENCES

Abuelizz, H. A., Marzouk, M., Bakhiet, A., Abdel-Aziz, M. M., Ezzeldin, E., Rashid, H., et al. (2021). In Silico study and Biological Screening of Benzoquinazolines as Potential Antimicrobial Agents against Methicillin-Resistant *Staphylococcus aureus*, Carbapenem-Resistant *Klebsiella pneumoniae*, and Fluconazole-Resistant Candida Albicans. *Microb. Pathogenesis* 160, 105157. doi:10.1016/j.micpath.2021.105157

Ahmad, F., and Zhou, Y. (2017). Pitfalls and Challenges in Nanotoxicology: a Case of Cobalt Ferrite (CoFe2O4) Nanocomposites. *Chem. Res. Toxicol.* 30, 492–507. doi:10.1021/acs.chemrestox.6b00377

Ahmed, S., SaifullahAhmad, M., Ahmad, M., Swami, B. L., and Ikram, S. (2016). Green Synthesis of Silver Nanoparticles Using Azadirachta indica Aqueous Leaf Extract. *J. Radiat. Res. Appl. Sci.* 9, 1–7. doi:10.1016/j.jrras.2015.06.006

Arakha, M., Pal, S., Samantarrai, D., Panigrahi, Tk., Mallick, Bc., Pramanik, K., et al. (2015). Antimicrobial Activity of Iron Oxide Nanoparticle upon Modulation of Nanoparticle-Bacteria Interface. *Sci. Rep.* 5, 1–12. doi:10.1038/srep14813

Ashraf, Jm., Ansari, Ma., Khan, Hm., Alzohairy, Ma., and Choi, I. (2016). Green Synthesis of Silver Nanoparticles and Characterization of Their Inhibitory Effects on AGEs Formation Using Biophysical Techniques. *Sci. Rep.* 6, 1–10. doi:10.1038/srep20414

Aunkor, M. T. H., Raihan, T., Prodhan, S. H., Metselaar, H. S. C., Malik, S. U. F., and Azad, A. K. (2020). Antibacterial Activity of Graphene Oxide Nanosheet against Multidrug Resistant Superbugs Isolated from Infected Patients. *R. Soc. Open Sci.* 7, 200640. doi:10.1098/rsos.200640

Bélteky, P., Rónavári, A., Igaz, N., Szerencsés, B., Tóth, I. Y., Pfeiffer, I., et al. (2019). Silver Nanoparticles: Aggregation Behavior in Biorelevant Conditions and its Impact on Biological Activity. *Ijn* Vol. 14, 667–687. doi:10.2147/ijn.s185965

Bharadwaj, K. K., Rabha, B., Pati, S., Choudhury, B. K., Sarkar, T., Gogoi, S. K., et al. (2021). Green Synthesis of Silver Nanoparticles Using Diospyros Malabarica Fruit Extract and Assessments of Their Antimicrobial, Anticancer and Catalytic Reduction of 4-Nitrophenol (4-NP). *Nanomaterials (Basel)* 11. doi:10.3390/nano11081999

Braine, T. (2011). Race against Time to Develop New Antibiotics. *Bull. World Health Organ.* 89, 88–89. doi:10.2471/BLT.11.030211

Chai, S.-H., Wang, Y., Qiao, Y., Wang, P., Li, Q., Xia, C., et al. (2018). Bio Fabrication of Silver Nanoparticles as an Effective Wound Healing Agent in the Wound Care after Anorectal Surgery. *J. Photochem. Photobiol. B: Biol.* 178, 457–462. doi:10.1016/j.jphotobiol.2017.10.024

da SilveiraCavalcante, L., Acker, J. P., and Holovati, J. L. (2015). Differences in Rat and Human Erythrocytes Following Blood Component Manufacturing: the Effect of Additive Solutions. *Transfus. Med. Hemother* 42, 150–157. doi:10.1159/000371474

de Oliveira, J. F. A., and Cardoso, M. B. (2014). Partial Aggregation of Silver Nanoparticles Induced by Capping and Reducing Agents Competition. *Langmuir* 30, 4879–4886. doi:10.1021/la403635c

Dhau, J. S., Singh, A., Brandão, P., and Felix, V. (2021). Synthesis, Characterization, X-ray crystal Structure and Antibacterial Activity of Bis[3-(4-Chloro-N,n-Diethylpyridine-2-Carboxamide)] Diselenide. *Inorg. Chem. Commun.* 133, 108942. doi:10.1016/j.inoche.2021.108942

Durán, N., Durán, M., De Jesus, M. B., Seabra, A. B., Fávaro, W. J., and Nakazato, G. (2016). Silver Nanoparticles: A New View on Mechanistic Aspects on Antimicrobial Activity. *Nanomedicine: Nanotechnology, Biol. Med.* 12, 789–799. doi:10.1016/j.nano.2015.11.016

Elamawi, R. M., Al-Harbi, R. E., and Hendi, A. A. (2018). Biosynthesis and Characterization of Silver Nanoparticles Using Trichoderma Longibrachiatum and Their Effect on Phytopathogenic Fungi. *Egypt. J. Biol. Pest Control* 28, 1–11. doi:10.1186/s41938-018-0028-1

Gajbhiye, S., and Sakharwade, S. (2016). Silver Nanoparticles in Cosmetics. *Jcdsa* 06, 48–53. doi:10.4236/jcdsa.2016.61007

Ghosh, A., Sarmah, P., Patel, H., Mukerjee, N., Mishra, R., Alkahtani, S., et al. (2022). Nonlinear Molecular Dynamics of Quercetin in Gynocardia Odorata and Diospyros Malabarica Fruits: Its Mechanistic Role in Hepatoprotection. *PLoS One* 17, e0263917. doi:10.1371/journal.pone.0263917

Goudarzi, M., Mir, N., Mousavi-Kamazani, M., Bagheri, S., and Salavati-Niasari, M. (2016). Biosynthesis and Characterization of Silver Nanoparticles Prepared from Two Novel Natural Precursors by Facile thermal Decomposition Methods. *Sci. Rep.* 6, 1–13. doi:10.1038/srep32539

Han, H., Zhu, J., Wu, D. Q., Li, F. X., Wang, X. L., Yu, J. Y., et al. (2019). Inherent Guanidine Nanogels with Durable Antibacterial and Bacterially Antiadhesive Properties. *Adv. Funct. Mater.* 29, 1806594. doi:10.1002/adfm.201806594

Haq, S. H., Al-Ruwaished, G., Naji, S. A., Al-Mogren, M., Al-Rashed, S., Ain, Q. T., et al. (2019). Antioxidant, Anticancer Activity and Phytochemical Analysis of Green Algae, Chaetomorpha Collected from the Arabian Gulf. *Sci. Rep.* 9, 18906. doi:10.1038/s41598-019-55309-1

He, Y., Du, Z., Ma, S., Liu, Y., Li, D., Huang, H., et al. (2016). Effects of green-synthesized Silver Nanoparticles on Lung Cancer Cells *In Vitro* and Grown as Xenograft Tumors *In Vivo*. *Ijn* 11, 1879–1887. doi:10.2147/ijn.s103695

Hindi, K. M., Ditto, A. J., Panzner, M. J., Medvetz, D. A., Han, D. S., Hovis, C. E., et al. (2009). The Antimicrobial Efficacy of Sustained Release Silver-Carbene Complex-Loaded L-Tyrosine Polyphosphate Nanoparticles: Characterization, *In Vitro* and *In Vivo* Studies. *Biomaterials* 30, 3771–3779. doi:10.1016/j.biomaterials.2009.03.044

Hoseinnejad, M., Jafari, S. M., and Katouzian, I. (2018). Inorganic and Metal Nanoparticles and Their Antimicrobial Activity in Food Packaging Applications. *Crit. Rev. Microbiol.* 44, 161–181. doi:10.1080/1040841x.2017.1332001

Hossain, M. M., Polash, S. A., Takikawa, M., Shubhra, R. D., Saha, T., Islam, Z., et al. (2019). Investigation of the Antibacterial Activity and *In Vivo* Cytotoxicity of Biogenic Silver Nanoparticles as Potent Therapeutics. *Front. Bioeng. Biotechnol.* 7, 239. doi:10.3389/fbioe.2019.00239

Kaegi, R., Voegelin, A., Sinnet, B., Zuleeg, S., Hagendorfer, H., Burkhardt, M., et al. (2011). Behavior of Metallic Silver Nanoparticles in a Pilot Wastewater Treatment Plant. *Environ. Sci. Technol.* 45, 3902–3908. doi:10.1021/es1041892

Kaur, B., Khera, A., and Sandhir, R. (2012). Attenuation of Cellular Antioxidant Defense Mechanisms in Kidney of Rats Intoxicated with Carbofuran. *J. Biochem. Mol. Toxicol.* 26, 393–398. doi:10.1002/jbt.21433

Kausar, F., Farooqi, M. A., Farooqi, H. M., Salih, A. R., Khalil, A. A., Kang, C. W., et al. (2021). Phytochemical Investigation, Antimicrobial, Antioxidant and Anticancer Activities of Acer Cappadocicum Gled. *Life (Basel)* 11. doi:10.3390/life11070656

Kim, D. H., Kim, K. N., Kim, K. M., Shim, I. B., and Lee, Y. K. (2007). *In Vitro* & *In Vivo* Toxicity of CoFe2O4 for Application to Magnetic Hyperthermia. *TechConnect Briefs* 2, 748–751. NSTI Nanotechnology Conference and Trade Show-NSTI Nanotech 2007.

Kim, T., Braun, G. B., She, Z.-G., Hussain, S., Ruoslahti, E., and Sailor, M. J. (2016). Composite Porous Silicon-Silver Nanoparticles as Theranostic Antibacterial Agents. *ACS Appl. Mater. Inter.* 8, 30449–30457. doi:10.1021/acsami.6b09518

Król, A., Pomastowski, P., Rafińska, K., Railean-Plugaru, V., and Buszewski, B. (2017). Zinc Oxide Nanoparticles: Synthesis, Antiseptic Activity and Toxicity Mechanism. *Adv. Colloid Interf. Sci.* 249, 37–52. doi:10.1016/j.cis.2017.07.033

Kruk, T., Szczepanowicz, K., Stefańska, J., Socha, R. P., and Warszyński, P. (2015). Synthesis and Antimicrobial Activity of Monodisperse Copper Nanoparticles. *Colloids Surf. B: Biointerfaces* 128, 17–22. doi:10.1016/j.colsurfb.2015.02.009

Levard, C., Hotze, E. M., Lowry, G. V., and Brown, G. E., Jr. (2012). Environmental Transformations of Silver Nanoparticles: Impact on Stability and Toxicity. *Environ. Sci. Technol.* 46, 6900–6914. doi:10.1021/es2037405

Li, W.-R., Xie, X.-B., Shi, Q.-S., Zeng, H.-Y., Ou-Yang, Y.-S., and Chen, Y.-B. (2010). Antibacterial Activity and Mechanism of Silver Nanoparticles on *Escherichia coli*. *Appl. Microbiol. Biotechnol.* 85, 1115–1122. doi:10.1007/s00253-009-2159-5

Li, X., Robinson, S. M., Gupta, A., Saha, K., Jiang, Z., Moyano, D. F., et al. (2014). Functional Gold Nanoparticles as Potent Antimicrobial Agents against Multi-Drug-Resistant Bacteria. *ACS nano* 8, 10682–10686. doi:10.1021/nn5042625

Li, Y., Zhang, W., Niu, J., and Chen, Y. (2012). Mechanism of Photogenerated Reactive Oxygen Species and Correlation with the Antibacterial Properties of Engineered Metal-Oxide Nanoparticles. *ACS nano* 6, 5164–5173. doi:10.1021/nn300934k

Masum, M. M. I., Siddiqa, M. M., Ali, K. A., Zhang, Y., Abdallah, Y., Ibrahim, E., et al. (2019). Biogenic Synthesis of Silver Nanoparticles Using Phyllanthus Emblica Fruit Extract and its Inhibitory Action against the Pathogen Acidovorax Oryzae Strain RS-2 of rice Bacterial Brown Stripe. *Front. Microbiol.* 10, 820. doi:10.3389/fmicb.2019.00820

Mathur, P., Jha, S., Ramteke, S., and Jain, N. K. (2018). Pharmaceutical Aspects of Silver Nanoparticles. *Artif. Cell Nanomedicine, Biotechnol.* 46, 115–126. doi:10.1080/21691401.2017.1414825

Mondal, R., Polash, S. A., Saha, T., Islam, Z., Sikder, M. M., Alam, N., et al. (2017). Investigation of the Phytoconstituents and Bioactivity of Various Parts of Wild Type and Cultivated <i>Phyllanthus Emblica</i> L. *Abb* 08, 211–227. doi:10.4236/abb.2017.87016

Mujeeb, F., Bajpai, P., and Pathak, N. (20142014). Phytochemical Evaluation, Antimicrobial Activity, and Determination of Bioactive Components from

Leaves of Aegle Marmelos. *Biomed. Res. Int.* 2014, 497606. doi:10.1155/2014/497606

Nayak, D., Ashe, S., Rauta, P. R., Kumari, M., and Nayak, B. (2016). Bark Extract Mediated green Synthesis of Silver Nanoparticles: Evaluation of Antimicrobial Activity and Antiproliferative Response against Osteosarcoma. *Mater. Sci. Eng. C* 58, 44–52. doi:10.1016/j.msec.2015.08.022

Niloy, M. S., Hossain, M. M., Takikawa, M., Shakil, M. S., Polash, S. A., Mahmud, K. M., et al. (2020). Synthesis of Biogenic Silver Nanoparticles Using Caesalpinia Digyna and Investigation of Their Antimicrobial Activity and *In Vivo* Biocompatibility. *ACS Appl. Bio Mater.* 3, 7722–7733. doi:10.1021/acsabm.0c00926

Polash, S. A., Khare, T., Kumar, V., and Shukla, R. (2021). Prospects of Exploring the Metal-Organic Framework for Combating Antimicrobial Resistance. *ACS Appl. Bio Mater.* 4, 8060–8079. doi:10.1021/acsabm.1c00832

Polash, S. A., Saha, T., Hossain, M. S., and Sarker, S. R. (2017a). Investigation of the Phytochemicals, Antioxidant, and Antimicrobial Activity of the <i> Andrographis Paniculata</i> Leaf and Stem Extracts. *Abb* 08, 149–162. doi:10.4236/abb.2017.85012

Polash, S. A., Saha, T., Hossain, M. S., and Sarker, S. R. (2017b). Phytochemical Contents, Antioxidant and Antibacterial Activity of the Ethanolic Extracts of *Centella asiatica*(L.) Urb.Leaf and Stem. *Jahangirnagar Univ. J. Biol. Sci.* 6, 51–57. doi:10.3329/jujbs.v6i1.33731

Poulose, S., Panda, T., Nair, P. P., and Théodore, T. (2014). Biosynthesis of Silver Nanoparticles. *J. Nanosci. Nanotech.* 14, 2038–2049. doi:10.1166/jnn.2014.9019

Ramaiah, S. K. (2007). A Toxicologist Guide to the Diagnostic Interpretation of Hepatic Biochemical Parameters. *Food Chem. Toxicol.* 45, 1551–1557. doi:10.1016/j.fct.2007.06.007

Ramalingam, B., Parandhaman, T., and Das, S. K. (2016). Antibacterial Effects of Biosynthesized Silver Nanoparticles on Surface Ultrastructure and Nanomechanical Properties of Gram-Negative Bacteria Viz. *Escherichia coli* and *Pseudomonas aeruginosa*. *ACS Appl. Mater. Inter.* 8, 4963–4976. doi:10.1021/acsami.6b00161

Ranjan Sarker, S., Polash, S. A., Boath, J., Kandjani, A. E., Poddar, A., Dekiwadia, C., et al. (2019). Functionalization of Elongated Tetrahexahedral Au Nanoparticles and Their Antimicrobial Activity Assay. *ACS Appl. Mater. Inter.* 11, 13450–13459. doi:10.1021/acsami.9b02279

Rao, K. J., and Paria, S. (2015). Aegle Marmelos Leaf Extract and Plant Surfactants Mediated green Synthesis of Au and Ag Nanoparticles by Optimizing Process Parameters Using Taguchi Method. *ACS Sustainable Chem. Eng.* 3, 483–491. doi:10.1021/acssuschemeng.5b00022

Sánchez-López, E., Gomes, D., Esteruelas, G., Bonilla, L., Lopez-Machado, A. L., Galindo, R., et al. (2020). Metal-Based Nanoparticles as Antimicrobial Agents: An Overview. *Nanomaterials (Basel)* 10. doi:10.3390/nano10020292

Sarker, S. R., Polash, S. A., Karim, M. N., Saha, T., Dekiwadia, C., Bansal, V., et al. (2022). Functionalized Concave Cube Gold Nanoparticles as Potent Antimicrobial Agents against Pathogenic Bacteria. *ACS Appl. Bio Mater.* 5, 492–503. doi:10.1021/acsabm.1c00902

Shriram, V., Khare, T., Bhagwat, R., Shukla, R., and Kumar, V. (2018). Inhibiting Bacterial Drug Efflux Pumps via Phyto-Therapeutics to Combat Threatening Antimicrobial Resistance. *Front. Microbiol.* 9, 2990. doi:10.3389/fmicb.2018.02990

Shubhra, R. D., Polash, S. A., Hossain, M. M., Hamza, A., Tushar, M. M. H., Saha, T., et al. (2021). Investigation of the Antimicrobial Activity and <i>*In Vivo* </i> Cytotoxicity of <i>Diospyros Malabarica </i> (Desr.) Kostel. Fruit Extracts. *Ns* 13, 331–351. doi:10.4236/ns.2021.138026

Shubhra, R. D., Polash, S. A., Saha, T., Hasan, A., Hossain, S., Islam, Z., et al. (2019). Investigation of the Phytoconstituents and Antioxidant Activity of <i> Diospyros Malabarica</i> Fruit Extracts. *Abb* 10, 431–454. doi:10.4236/abb.2019.1012031

Singh, A., Kaushik, A., Dhau, J. S., and Kumar, R. (2022). Exploring Coordination Preferences and Biological Applications of Pyridyl-Based Organochalcogen (Se, Te) Ligands. *Coord. Chem. Rev.* 450, 214254. doi:10.1016/j.ccr.2021.214254

Wang, L., Hu, C., and Shao, L. (2017). The Antimicrobial Activity of Nanoparticles: Present Situation and Prospects for the Future. *Ijn* 12, 1227–1249. doi:10.2147/ijn.s121956

Zhang, Y., Shareena Dasari, T. P., Deng, H., and Yu, H. (2015). Antimicrobial Activity of Gold Nanoparticles and Ionic Gold. *J. Environ. Sci. Health C* 33, 286–327. doi:10.1080/10590501.2015.1055161

Conflict of Interest: The authors declare that the research was conducted in the absence of any commercial or financial relationships that could be construed as a potential conflict of interest.

Publisher's Note: All claims expressed in this article are solely those of the authors and do not necessarily represent those of their affiliated organizations, or those of the publisher, the editors and the reviewers. Any product that may be evaluated in this article, or claim that may be made by its manufacturer, is not guaranteed or endorsed by the publisher.